ELSEVIER

J. Non-Newtonian Fluid Mech. 95 (2000) 55–65

Journal of Non-Newtonian Fluid Mechanics

www.elsevier.com/locate/jnnfm

A traceless stress tensor formulation for viscoelastic fluid flow

Paulo J. Oliveira*

Departamento de Engenharia Electromecânica, Universidade da Beira Interior, 6200 Covilhã, Portugal

Received 18 May 2000; received in revised form 17 July 2000

Abstract

A novel formulation of the differential equations governing the flow of viscoelastic fluids is proposed, based on the use of the traceless stress tensor (TST). It is shown that it naturally leads to the appearance of a modified viscosity given by $\eta + (\lambda/3) \cdot \mathrm{tr}(\tau)$ where η is the shear-viscosity coefficient, λ the relaxation time and $\mathrm{tr}(\tau)$ the trace of the extra stress tensor. This modified viscosity reaches high values near singular points, the troublesome regions when solving numerically the equations, and therefore its inclusion will tend to stabilise the computations when the modified-viscous terms in the momentum equations are treated implicitly.

Keywords: Traceless tensor; Viscoelastic; UCM; Differential formulation; Numerical method

1. Introduction

In this paper, we present a new idea for the formulation of the differential equations governing the flow of viscoelastic fluids, aimed at enhancing the stability of the numerical methods used to solve those equations when the levels of elasticity are high. This idea will be most useful in conjunction with decoupled numerical methods, like the finite-volume type of methods (FVM) that the present author and colleagues have been developing [1], but is also applicable to finite-element methods (FEM) and other FV methods, as we shall discuss. In particular, it can be directly applied to adaptive-viscosity methods which are becoming increasingly popular.

We are thus dealing (indirectly) with the so-called high Weissenberg number problem (see Keunnings [2] and Crochet [3]), whereby numerical solution of viscoelastic flows becomes more and more difficult as the Weissenberg (*We*) number increases. During the past 13 years significant progress has been made regarding this matter and it is now accepted that the difficulties of computing high-*We* flows are numerical and not related to the mathematical well-posedness of the starting equations, e.g. [2,4,5]. In a recent review, Renardy [5] refers to "well-posed iteration and discretisation schemes" (in contrast to well-posed equations) as being crucial for successful numerical methods.

* Fax: +351-275-320820.
E-mail address: pjpo@ubi.pt (P.J. Oliveira).

0377-0257/00/$ – see front matter
PII: S0377-0257(00)00164-6

The efforts to mitigate the high-Weissenberg number problem have been of two types: either (1) by re-arranging the starting differential equations in such a way that the new set, although mathematically equivalent to the original, possesses better characteristics for the numerical solution methods (the momentum equations become more "elliptic"); or (2) by improving the numerics of the specific methods used to solve the equations. Most numerical procedures found in the literature for visco elastic flow are of the finite-element type, except in the early years of computational rheology, e.g. Davies et al. [6] (a certain tendency for change is just emerging: Sasmal [7]; Xue et al. [8]; Oliveira et al. [1]). One of the first important breakthroughs on FEM was made by Marchal and Crochet [9] in 1987. Their contribution falls on the second type above: introduction of a form of streamline upwinding in the discretisation of the constitutive equation and use of differing elements for the different variables — quadratic for velocity and linear for pressure and stresses (with 4×4 sub-elements). Marchal and Crochet implemented the proposed improvements in a FEM code and applied it with considerable success to a number of typically difficult flows, slip-stick, contraction flows, etc. obtaining solutions at much higher *We* than before. Later, a number of contributions also fell in that second type: Fortin and Fortin [10] — discontinuous interpolation and decoupled schemes; Sato and Richardson [11] — mixed FV + FE techhiques; Webster and coworkers [12,13] — FEM with pressure-correction techniques borrowed from FVM and reconstruction of smoother velocity gradients for the constitutive equation; Sun et al. [14] — recent work incorporating various FEM techniques including discontinuous Galerkin approximations for the stresses and least squares interpolation for the velocity gradients.

Typical examples of efforts of the first type are the formulations known as the elastic viscous split stress (EVSS) and the explicit elliptic momentum equation (EEME). EVSS is usually referred to Rajagopalan et al. [15] in the context of FEM, but the basic idea which interests us most was quite evident (in retrospect) and in fact was used long before, e.g. by Perera and Walters [16]. The outcome of EVSS is that a fully viscous term appears in the momentum equation (even for a constitutive model devoid of solvent viscosity, as the upper-convected Maxwell UCM) thus increasing the ellipticity of that equation. Those viscous terms are treated implicitly in FEM or FVM methods and thus tend to stabilize any of the numerical methods when some form of iteration is utilized.

A somewhat different form of EVSS has recently been introduced by Sun et al. [17] who coined it the AVSS, standing for adaptive viscoelastic stress splitting. In this case the added viscous terms in the momentum equation use an artificial viscosity which varies in the field in such a way that will be highest in zones of higher stresses, thus promoting stability (through ellipticity). The expressions adopted for the adaptive viscosity are purely empirical, based on numerical experiments, and in the original paper it was estimated by assuming that the magnitude of the viscous and elastic stresses were the same, yielding: $\alpha h \tau_{\max}/u_{\max}$, where the constant $\alpha \approx 1$ and h is a characteristic size of the finite elements. The maximum values of stresses and velocity, $\tau_{\max}$ and $u_{\max}$, have to be found throughout the flow domain. In more recent form of AVSS (e.g. [14]) the expressions to calculate the adaptive viscosity are more elaborate but their basis continues to be empirical.

The explicitly elliptic momentum equation (EEME) formulation of King et al. [18] also relies on a manipulation of the momentum, continuity and constitutive equations such that the newly obtained momentum equation becomes more "elliptic" (more terms treated implicitly and included into the Laplacian operator). It has been implemented in FEM and shown to yield good results in a number of cases [18] but it is fair to say that the modified equations are in terms of the vorticity $\omega = \nabla \times u$, a variable which is problematic, especially near solid walls (Roache [19]), and has long lost favour in classic CFD with Newtonian fluids — in fact the old vorticity-streamfunction formulation has practically been replaced

by the primitive variables velocity–pressure. Furthermore, this formulation is restricted to flows without inertia (zero Reynolds number).

The formulation we propose here is based on the use of the traceless stress tensor (TST), that is the deviatoric part of the stress obtained from subtraction of the trace to the original tensor. The idea was originated from observations in Newtonian calculations with incompressible fluids and the FVM in non-staggered meshes, in which we have noticed that if the stress is forced to be traceless (as they are in the differential formulation) then not only the resulting solution was more smooth (so better results) but the number of iterations to obtain those results would be much less, e.g. [20]. Like the EEME, our proposal entails a reformulation of the governing equations but whereas in EEME that is restricted to the momentum equation, here the constitutive equation is also modified. In fact, the present formulation brings part of the stresses from the constitutive equation into the momentum equation, therefore tightening the coupling between those equations. The derivation and consequences of adopting a TST formulation are examined in the Sections 2 and 3 in the context of the upper-convected Maxwell model. It will be shown that an "artificial viscosity" naturally arises and this can be very useful for the AVSS type of methods. A generalisation to the Phan-Thien–Tanner model is given in Section 4, and some preliminary results supporting the method in Section 5.

2. Traceless formulation for the UCM

Incompressible fluid flow is governed by the continuity and momentum equations:

$$\frac{\partial u_j}{\partial x_j} = 0, \tag{1}$$

$$\frac{\partial \rho u_i}{\partial t} + \frac{\partial \rho u_j u_i}{\partial x_j} = \frac{\partial \sigma_{ij}}{\partial x_j} + \rho g_i, \tag{2}$$

where u_i and σ_{ij} are the components on a Cartesian frame x_i of the velocity vector and stress tensor, respectively, t the time, ρ the fluid density and g_i a body-force acceleration (typically due to gravity). The Cauchy total stress tensor σ_{ij} can be decomposed into a "pressure" contribution plus a deviatoric stress, as in the following equation:

$$\sigma_{ij} = -p'\delta_{ij} + \left(\tau_{ij} - \tfrac{1}{3}\tau_{kk}\delta_{ij}\right), \tag{3}$$

where δ_{ij} is the Kronecker delta and the trace of the extra stress τ_{ij}, $\tau_{kk} \equiv \mathrm{tr}(\tau)$, may generally be different from zero. For this reason we denote the pressure in Eq. (3) with p' to emphasise that it will be different from the usual pressure defined from the standard decomposition:

$$\sigma_{ij} = -p\delta_{ij} + \tau_{ij}. \tag{4}$$

Two alternative formulations are possible when one seeks to solve numerically the above equations. In the first, the trace of the stress tensor is separated from the divergence term and added to the pressure gradient leading to the following form of the momentum equation:

$$\frac{\partial \rho u_i}{\partial t} + \frac{\partial \rho u_j u_i}{\partial x_j} = -\frac{\partial (p' + (1/3)\tau_{kk})}{\partial x_i} + \frac{\partial \tau_{ij}}{\partial x_j} + \rho g_i. \tag{5}$$

Clearly, if we denote $p \equiv p' + (1/3)\tau_{kk}$ (from Eqs. (3) and (4)), then Eq. (5) is nothing but the usual momentum equation found in most works in the literature whereby one solves for p and τ_{ij}. More interesting is the second formulation in which we keep working with p' and the traceless tensor. In this case, if we insert Eq. (3) into (2), we obtain

$$\frac{\partial \rho u_i}{\partial t} + \frac{\partial \rho u_j u_i}{\partial x_j} = -\frac{\partial p'}{\partial x_i} + \frac{\partial(\tau_{ij} - (1/3)\tau_{kk}\delta_{ij})}{\partial x_j} + \rho g_i, \tag{6}$$

which can also be written as

$$\frac{\partial \rho u_i}{\partial t} + \frac{\partial \rho u_j u_i}{\partial x_j} = -\frac{\partial p'}{\partial x_i} + \frac{\partial \tau'_{ij}}{\partial x_j} + \rho g_i, \tag{7}$$

where τ'_{ij} is the traceless tensor defined by

$$\tau'_{ij} \equiv \tau_{ij} - \tfrac{1}{3}\tau_{kk}\delta_{ij}. \tag{8}$$

In this section, the basic idea of our proposal is explained by taking as rheological constitutive law the upper-convected Maxwell model (UCM). This is one of the simplest differential viscoelastic fluid models but nonetheless one that is connoted as giving rise to the greatest numerical difficulties, e.g. [3,4,8,9,12,13]. Since our proposal is aimed at improving the numerics in viscoelastic flow calculations, it makes sense to look first at the most difficult model. In the UCM model the extra stress is purely viscoelastic — there is no solvent viscosity — and its evolution is governed by the following constitutive equation (Bird et al. [21]):

$$\tau_{ij} + \lambda \frac{\mathrm{D}\tau_{ij}}{\mathrm{D}t} = \eta\left(\frac{\partial u_i}{\partial x_j} + \frac{\partial u_j}{\partial x_i}\right) + \lambda\left(\tau_{ik}\frac{\partial u_j}{\partial x_k} + \tau_{jk}\frac{\partial u_i}{\partial x_k}\right), \tag{9}$$

where the two constants λ and η are the relaxation time and the viscosity coefficient, respectively. We note that part of Oldroyd's upper convected derivative has been shifted to the right hand side of the equation (term multiplied by λ). This term may be seen as representing generation of stress by interaction with the velocity gradients, in analogy to the equivalent vortex-strechting term in standard turbulence models (the so-called production or generation term), and is usually treated explicitly in an iterative solution procedure (in passing, it should be said that strong similarities between laminar flow of viscoelastic fluids and turbulent flows of Newtonian fluids have been recognised for a long time, e.g. Rivlin [22]). It is quite clear by contracting indices that the trace of τ_{ij} is not zero and evolves with the flow. The question now is how to incorporate this stress equation with the momentum balance, and this requires a choice among the possible forms represented by Eqs. (5)–(7).

Eq. (5) leads to the standard practice for the momentum equation, as noted above. In Section 1 we argue for the use of the traceless stress tensor and there are two ways of implementing this traceless stress approach. The first and more obvious is to work with Eq. (6) and retain the original constitutive Eq. (9). In this way, this last equation is solved for τ_{ij} but it is the traceless stress tensor that is then utilised in the momentum Eq. (6), with p' instead of the usual p. This approach offers some potential advantages when applied in conjunction with a finite-volume method in non-staggered meshes and will be explored in future work, but it is not the proposed approach. What we advocate for is to follow Eq. (7) and hence to entirely adopt the traceless tensor and, consequently, the constitutive equation will have to be expressed

in terms of τ'. To do this, τ_{ij} from Eq. (8) is inserted into Eq. (9) to obtain

$$\left(\tau'_{ij}+\frac{1}{3}\tau_{kk}\delta_{ij}\right)+\lambda\frac{\mathrm{D}(\tau'_{ij}+(1/3)\tau_{kk}\delta_{ij})}{\mathrm{D}t}=\eta\left(\frac{\partial u_i}{\partial x_j}+\frac{\partial u_j}{\partial x_i}\right)+\lambda\left(\left(\tau'_{ik}+\frac{1}{3}\tau_{ll}\delta_{ik}\right)\frac{\partial u_j}{\partial x_k}+\left(\tau'_{jk}+\frac{1}{3}\tau_{ll}\delta_{jk}\right)\frac{\partial u_i}{\partial x_k}\right).$$

This expression, after some rearrangement and by noting that $\delta_{ik}\partial u_j/\partial x_k=\partial u_j/\partial x_i$, etc. from contraction of indices, leads to

$$\tau'_{ij}+\lambda\frac{\mathrm{D}\tau'_{ij}}{\mathrm{D}t}=\left(\eta+\frac{\lambda}{3}\tau_{kk}\right)\left(\frac{\partial u_i}{\partial x_j}+\frac{\partial u_j}{\partial x_i}\right)+\lambda\left(\tau'_{ik}\frac{\partial u_j}{\partial x_k}+\tau'_{jk}\frac{\partial u_i}{\partial x_k}\right)-\frac{1}{3}\left(\tau_{kk}+\lambda\frac{\mathrm{D}\tau_{kk}}{\mathrm{D}t}\right)\delta_{ij}. \quad (10)$$

In order to use this equation we need a relation governing the evolution of τ_{kk}. This may be directly obtained from the original Eq. (9) by contracting indices, to yield

$$\tau_{kk}+\lambda\frac{\mathrm{D}\tau_{kk}}{\mathrm{D}t}=2\eta\frac{\partial u_k}{\partial x_k}+2\lambda G, \quad (11)$$

where the G-term, by analogy to the generation term in turbulence modelling, stands for

$$G\equiv\tau_{jk}\frac{\partial u_j}{\partial x_k}.$$

Since this G-term is still expressed with the original stress components there is the need again to substitute in this last expression τ', for τ, by using Eq. (8), to obtain

$$G=\tau'_{jk}\frac{\partial u_j}{\partial x_k}+\frac{1}{3}\tau_{kk}\frac{\partial u_j}{\partial x_j}=G'+\frac{1}{3}\tau_{kk}\frac{\partial u_j}{\partial x_j}, \quad (12)$$

where the G'-term is now based on the traceless stress components, which are the main dependent stress variables:

$$G'\equiv\tau'_{jk}\frac{\partial u_j}{\partial x_k}. \quad (13)$$

The evolution of the trace can then be written as

$$\tau_{kk}+\lambda\frac{\mathrm{D}\tau_{kk}}{\mathrm{D}t}=2\left(\eta+\frac{\lambda}{3}\tau_{kk}\right)\frac{\partial u_k}{\partial x_k}+2\lambda G'. \quad (14)$$

It should be noted that terms involving the divergence of the velocity vector ($\partial u_k/\partial x_k$) are taken into account in the above equations in spite of the continuity constraint, Eq. (1), because the divergence is not exactly zero in many numerical approximations. This is particularly relevant in FVM with non-staggered meshes [20] in which the convective fluxes at cell faces do satisfy continuity exactly (to the tolerance imposed in the solution of the pressure-correction equation) but the cell-centred velocity field does not. If the numerical method used is such that the divergence of the velocity field is zero to the required tolerance (such as a FVM in a staggered mesh) than the terms in ($\partial u_k/\partial x_k$) may be omitted in the above equations. In any case, care should be taken to solve Eq. (14) with a velocity field satisfying continuity closely.

After multiplying Eq. (14) by $\delta_{ij}/3$ and introducing it into Eq. (10), we find the final expression for the τ' stress equation to be

$$\tau'_{ij} + \lambda \frac{\mathrm{D}\tau'_{ij}}{\mathrm{D}t} = \left(\eta + \frac{\lambda}{3}\tau_{kk}\right)\left(\frac{\partial u_i}{\partial x_j} + \frac{\partial u_j}{\partial x_i} - \frac{2}{3}\frac{\partial u_k}{\partial x_k}\delta_{ij}\right) + \lambda\left(\tau'_{ik}\frac{\partial u_j}{\partial x_k} + \tau'_{jk}\frac{\partial u_i}{\partial x_k}\right) - \frac{2}{3}\lambda G'\delta_{ij}. \tag{15}$$

This equation represents the UCM model in terms of a traceless extra stress tensor, τ'_{ij}. It may be readily confirmed that contraction of indices in Eq. (15) results in the identity $0 = 0$, reflecting the fact that trace of τ'_{ij} does vanish. It is also interesting to notice the appearance of the $-2/3$-term in the rate-of-deformation tensor as it is usually the case in a complete Newtonian formulation.

3. Discussion of the TST formulation for the UCM

By adopting the TST formulation we are able to obtain a tighter coupling between the flow and constitutive equations: a large part of the stress tensor (specifically, its trace) is now in the momentum equation (specifically, in the pressure gradient and diffusion term — see below) where it may be implicitly incorporated in a numerical scheme. The remarkable point about the new UCM equation for the traceless stress tensor, Eq. (15), and one which may have important implications in the numerical schemes, is the appearance of a modified viscosity multiplying the traceless strain rate tensor, namely

$$\eta' \equiv \eta + \frac{\lambda}{3}\tau_{kk}. \tag{16}$$

Since a viscosity is only meaningful if it is a positive quantity we, therefore, expect that the trace of τ is also always positive. This is indeed the case as can be inferred from Eq. (14), the hyperbolic equation governing the evolution of that quantity. If τ_{kk} is positive at the inlets to the flow domain, then Eq. (14) guarantees that τ_{kk} will remain positive provided the terms on the right hand side — the source terms — are either null (the first term) or positive definite (the second term). This is so because G' is the product of the traceless deviatoric stress tensor — which is symmetric — by the velocity gradient, representing the irreversible increase of internal energy of the fluid, a positive quantity according to the second law of thermodynamics (dissipation by viscosity).

This last assertion is not fully-proven by the existing theory for thermoviscoelasticity (cf. Bird and Curtiss [23]) and so it is relevant at this stage to see how τ_{kk} behaves in some actual typical flows. Instead of plotting directly τ_{kk} it is more instructive to plot $\eta'/\eta = 1 + \lambda\tau_{kk}/3\eta$, a modified normalised viscosity. For a UCM fluid, η is a constant and areas in the flow of η'/η much higher than one will be an indication of high τ_{kk}. Two flow configurations are examined: Fig. 1 shows isoplots in a 4:1 plane contraction flow (at Deborah number of $De = 2$, see [20]); and Fig. 2 shows isoplots for the flow produced by a cylinder falling in a channel, with a blockage ratio of 0.5 (at $De = 1$ and $Re = 1$, see [1]). These cases are based on results from numerical simulations with the finite-volume method. These figures confirm that τ_{kk} is indeed positive (η'/η is always >1) and, as expected, τ_{kk} becomes very large close to the singular point in the first test case, and around the cylinder and its wake in the second. As a consequence, the modified viscosity presents a large peak near the re-entrant corner in the contraction case of Fig. 1. In the second example (Fig. 2), classified as a smooth flow since there are no geometrical singular points, the modified viscosity is concentrated in the stress boundary layer on the cylinder surface and in the stress wake behind the cylinder — the problematic areas in the simulation of this problem [14,17]. These examples show

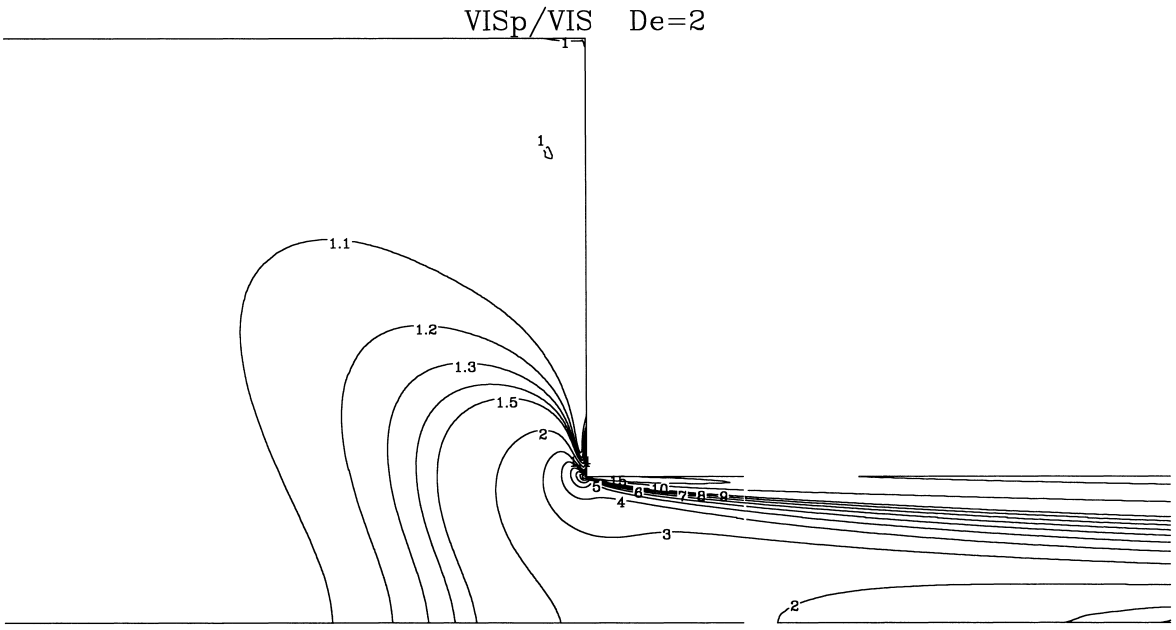

Fig. 1. Contours of the modified viscosity field η'/η in a plane sudden contraction at $De = 2$ (note: $(\eta'/\eta)_{\max} = 67.5$).

that if one can use the high values of the modified viscosity to profit, then one has a powerful means of stabilising the calculations near the problematic points. The way to do this is well known and falls in the EVSS formulation, as shown now.

The numerical scheme appropriate for the traceless stress tensor formulation should be based on implicit solution of the momentum equation, with the diffusive fluxes based on the increased viscosity η' and treated implicitly. We may do this directly by simply adding a diffusive term to both sides of the momentum Eq. (7), as

$$\frac{\partial \rho u_i}{\partial t} + \frac{\partial \rho u_j u_i}{\partial x_j} - \frac{\partial}{\partial x_j}\left(\eta' \frac{\partial u_i}{\partial x_j}\right) = -\frac{\partial p'}{\partial x_i} + \frac{\partial \tau'_{ij}}{\partial x_j} + \rho g_i - \frac{\partial}{\partial x_j}\left(\eta' \frac{\partial u_i}{\partial x_j}\right), \tag{17}$$

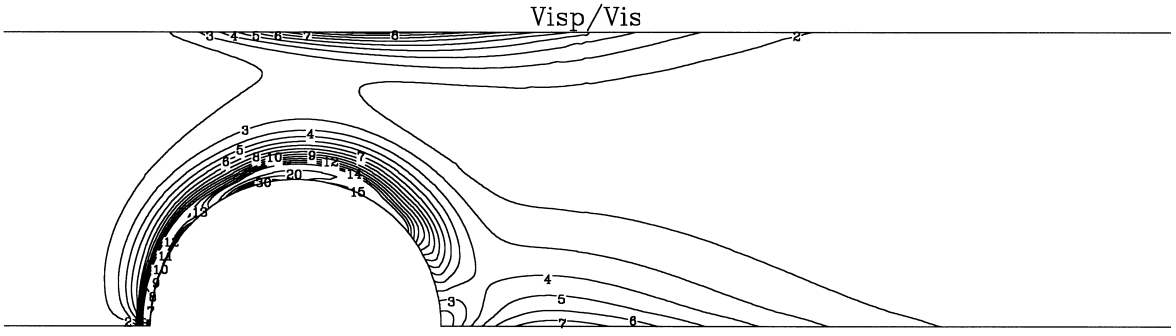

Fig. 2. Contours of the modified viscosity field in the flow around a cylinder, at $De = 1$ and $Re = 1$ (note: $(\eta'/\eta)_{\max} = 32.3$).

where the terms on the left-hand side are treated implicitly and those on the right-hand side are treated explicitly (that is, are included into the source term). Similar addition of diffusive terms has been done in our previous work [1] without any convergence problems and also by Perera and Walters [16] a long time ago. The proposal of Guenette and Fortin [24] is also, in essence, equivalent to using Eq. (17). Alternatively, we may use a form of the EVSS by splitting the traceless stress tensor as

$$\boldsymbol{\tau}' = \boldsymbol{\tau}'_1 + \boldsymbol{\tau}'_2, \tag{18}$$

with

$$\boldsymbol{\tau}'_2 = 2\eta' \boldsymbol{D}', \tag{19}$$

where D' is the traceless rate-of-strain tensor (the first term on the rhs of Eq. (15) multiplied by η'). The traceless stress tensor formulation (15) can be written in tensorial notation as

$$\boldsymbol{\tau}' + \lambda \overset{\nabla'}{\boldsymbol{\tau}'} = 2\eta' \boldsymbol{D}', \tag{20}$$

where we use the following modified definition for the upper convected derivative:

$$\overset{\nabla'}{\boldsymbol{\tau}'} = \frac{\mathrm{D}\boldsymbol{\tau}'}{\mathrm{D}t} - \left(\boldsymbol{\tau}' \cdot \boldsymbol{\nabla u} + \boldsymbol{\nabla u}^{\mathrm{T}} \cdot \boldsymbol{\tau}' - \frac{2}{3}(\boldsymbol{\tau}' : \boldsymbol{\nabla u})\boldsymbol{\delta} \right). \tag{21}$$

This differs from the usual definition by inclusion of the last term (the G'-term of Eq. (13)) which induces a vanishing result upon tensorial contraction. Since the operator in (21) is linear on τ', we may apply the decomposition (18) and introduce the two traceless tensors τ'_1 and τ'_2 into the momentum Eq. (7), to arrive at a result analogous to the EVSS:

$$\rho \frac{\mathrm{D}\boldsymbol{u}}{\mathrm{D}t} = -\boldsymbol{\nabla} p' + \boldsymbol{\nabla} \cdot \left(\eta' (\boldsymbol{\nabla u} + \boldsymbol{\nabla u}^{\mathrm{T}} - \frac{2}{3}(\boldsymbol{\nabla} \cdot \boldsymbol{u})\boldsymbol{\delta}) \right) + \boldsymbol{\nabla} \cdot \boldsymbol{\tau}'_1 + \rho g, \tag{22}$$

$$\boldsymbol{\tau}'_1 + \lambda \overset{\nabla'}{\boldsymbol{\tau}'_1} = -\lambda \overset{\nabla'}{\boldsymbol{\tau}'_2}, \tag{23}$$

where the term on the right-hand side of (23) contains only velocity gradients, like in the standard EVSS counterpart, e.g. [15]. The beneficial effects of the present formulation, besides the expected better pressure–velocity coupling due to use of p', will be felt through the diffusive term in the momentum Eq. (22) which is multiplied by the modified viscosity η'. Since that term is treated implicitly in the numerical procedure, there will be a tendency to enhanced stability whenever either λ or τ_{kk} increase, and therefore the schemes should behave well in problematic regions and at high *De*. The high Weissenberg number problem is thus expected to be greatly reduced (an expectation in-line with reported performance of AVSS methods).

4. Generalisation to other constitutive models

The traceless stress tensor formulation can be easily extended to other constitutive models and this is demonstrated here with the Phan-Thien–Tanner [25] equation:

$$f(\mathrm{tr}(\boldsymbol{\tau})) + \boldsymbol{\tau} + \lambda \overset{\nabla}{\boldsymbol{\tau}} = 2\eta \boldsymbol{D}, \tag{24}$$

where f is a function of the trace of stress tensor which can take the following forms:

$$f(\mathrm{tr}(\boldsymbol{\tau})) = 1 + \frac{\lambda\varepsilon}{\eta}\mathrm{tr}(\boldsymbol{\tau}) \quad \text{or} \quad f(\mathrm{tr}(\boldsymbol{\tau})) = \exp\left(\frac{\lambda\varepsilon}{\eta}\mathrm{tr}(\boldsymbol{\tau})\right).$$

This model has been widely used with both the linear and the exponential forms for the stress coefficient f and, comparatively to the UCM, shows a shear-thinning viscosity and a bounded elongational viscosity in a simple uniaxial stretching. It is also better behaved numerically thus allowing solution at higher Deborah numbers than the UCM.

If we substitute τ in Eq. (24) by the traceless tensor from Eq. (8) we end up with the following equation ($\tau_{kk} = \mathrm{tr}(\tau)$):

$$f(\tau_{kk})\boldsymbol{\tau}' + \lambda\frac{\mathrm{D}\boldsymbol{\tau}'}{\mathrm{D}t} = 2\left(\eta + \frac{\lambda}{3}\tau_{kk}\right)\boldsymbol{D} + \lambda\boldsymbol{G}' - \frac{1}{3}\left(f(\tau_{kk})\tau_{kk} + \lambda\frac{\mathrm{D}\tau_{kk}}{\mathrm{D}t}\right)\delta, \tag{25}$$

with

$$\boldsymbol{G}' = \boldsymbol{\tau}' \cdot \boldsymbol{\nabla u} + \boldsymbol{\nabla u}^{\mathrm{T}} \cdot \boldsymbol{\tau}',$$

noting that the scalar G' defined by Eq. (13) is twice the trace of the second-order tensor $\boldsymbol{G}'$. The evolution of the trace of τ is governed by an equation similar to (11), obtained by contraction of indices of (24):

$$f(\tau_{kk})\tau_{kk} + \lambda\frac{\mathrm{D}\tau_{kk}}{\mathrm{D}t} = 2\left(\eta + \frac{\lambda}{3}\tau_{kk}\right)D_{kk} + 2\lambda G'. \tag{26}$$

This equation can now be inserted into (25) to obtain

$$f(\tau_{kk})\boldsymbol{\tau}' + \lambda\frac{\mathrm{D}\boldsymbol{\tau}'}{\mathrm{D}t} = 2\left(\eta + \frac{\lambda}{3}\tau_{kk}\right)\left(\boldsymbol{D} - \frac{1}{3}D_{kk}\boldsymbol{\delta}\right) + \lambda\left(\boldsymbol{G}' - \frac{1}{3}G'_{kk}\boldsymbol{\delta}\right), \tag{27}$$

which can be written in a more compact form using the modified convected derivative of Eq. (21), the modified viscosity of Eq. (16), and the traceless deformation tensor D':

$$f(\tau_{kk})\boldsymbol{\tau}' + \lambda\overset{\nabla'}{\boldsymbol{\tau}'} = 2\eta'\boldsymbol{D}'. \tag{28}$$

Thus, the traceless form of the PTT equation is similar to the original equation and, again, we obtain an increased modified viscosity η' which contains part of the normal stresses of the original tensor. This increased diffusive term should be incorporated into the momentum equation and treated implicitly, following the procedures described in Section 4.

5. Some preliminary results

We give in this section some preliminary results from application of the present method in two simple flows of UCM fluids, with emphasis on possible improvements on numerical aspects of the resulting FVM code brought about by the method. A more comprehensive numerical study is left for a future work where a wider range of problems and parameters (*We*, *Re*, etc.) will be considered and issues like detailed mesh-refinement tests will be undertaken.

Table 1
Preliminary results for a channel flow

$We \equiv \lambda\dot{\gamma}_{wall}$	Standard method		Traceless method	
	Total pressure iter.	No. time steps	Total pressure iter.	No. time steps
0.3	3434	265	2193	265
0.6	6129	459	2428	460
0.9	8768	653	2316	657
1.2	10957	824	2163	826
1.5	12609	975	2080	999

First, we consider a developing plane channel flow at a Reynolds number of unity (based on average velocity and channel half-width), solved on a uniform 20×20 mesh for a channel aspect ratio of 10/1 (length/half-width), for which we obtain the results given in Table 1. The standard method is the finite volume procedure described in [1,20] in which a steady solution is obtained from a pseudo-time marching approach in a collocated mesh, using a decoupled scheme (the equations for momentum, pressure and stresses are solved sequentially, one after the other) and a pressure-correction technique. The traceless method was obtained after incorporating the formulation from Section 2 into the standard FV code. Table 1 gives the number of time steps to attain a steady solution (relative tolerance for the residuals of the equations of 10^{-4}), which is like the number of outer iterations, and the total number of inner iterations to solve the pressure-correction equation at all time steps. This is the important numerical parameter to look at, since most of the computational work is spent in solving the pressure equation, especially as the meshes are refined. Table 1 shows that the number of time steps (or outer iterations) increases with *We* but is more or less the same for the standard and the traceless method; however, the total number of iterations in the pressure solver increases substantially with the standard method and remains approximately constant with the new traceless method. At $We = 1.5$, the standard method requires six-times more pressure iterations than the traceless method, with consequent implications on the overall computing time.

Table 2 gives the same type of numerical results for the flow of a UCM fluid through a 4:1 plane contraction at a Reynolds number of unity (based on half-width of the small channel and average velocity there). Simulations with the standard and traceless code have been carried out on a medium mesh with 2960 non-uniform control volumes [20]. In order to guarantee the correctness of the traceless method implementation, some resulting physical features of the flow, such as length and intensity of the re-entrant corner recirculation, have been checked to be identical up to three digits accuracy. Again, Table 2 shows

Table 2
Preliminary results for a 4:1 plane contraction flow

$We \equiv \lambda\dot{\gamma}_{wall}$	Standard method		Traceless method	
	Total pressure iter.	No. time steps	Total pressure iter.	No. time steps
0.0	8641	798	–	–
0.3	2442	651	1859	651
0.6	4074	664	3008	663
1.2	6935	725	3711	803

that the traceless method requires substantially less iterations to solve the pressure-correction equation (a factor of 0.54 at $We = 1.2$) and, for the relative low *We* here considered, that reflects the effect of the modified pressure (Eq. (3)) in the velocity–pressure coupling.

6. Conclusions

A traceless stress tensor formulation for viscoelastic fluid flow is proposed and explained. It is shown that for both the UCM and PTT models this formulation leads to modified constitutive equations, Eqs. (15) and (28), respectively, with essentially the same structure as the original equations. However, the strain-rate term is multiplied by a modified viscosity, defined by Eq. (16), which will tend to be high in "problematic" zones. Indeed, if we write the modified viscosity in a non-dimensional form, it becomes equal to $1 + (De/3)\mathrm{tr}(\tau)$, and thus increases with elasticity ($De \uparrow$) and near singular points ($\mathrm{tr}(\tau) \uparrow$). Therefore, any numerical method designed to deal implicitly with the diffusion term in the momentum equation, based on the modified viscosity, will tend to have increased stability, in particular in the problematic regions where the modified viscosity is high. The modified viscosity of Eq. (16) may also be useful in AVSS type methods, instead of the current elaborate expressions for the adaptive viscosity, such as that of [14]. Preliminary results obtained in conjunction with a FVM indicate better pressure–velocity coupling due to use of the modified pressure p', with the traceless formulation requiring much less pressure iterations than the standard one.

References

[1] P.J. Oliveira, F.T. Pinho, G.A. Pinto, J. Non-Newtonian Fluid Mech. 79 (1998) 1–43.
[2] R. Keunings, J. Non-Newtonian Fluid Mech. 20 (1986) 209–226.
[3] M.J. Crochet, Numerical simulation of viscoelastic flow, Von Karman Lecture Series 1994-03 (1994).
[4] V. Warichet, V. Legat, J. Non-Newtonian Fluid Mech. 73 (1997) 95–114.
[5] M. Renardy, J. Non-Newtonian Fluid Mech. 90 (2000) 243–259.
[6] A.R. Davies, K. Walters, M.F. Webster, J. Non-Newtonian Fluid Mech. 4 (1979) 325–344.
[7] G.P. Sasmal, J. Non-Newtonian Fluid Mech. 56 (1995) 15–47.
[8] S.-C. Xue, N. Phan-Thien, R.I. Tanner, J. Non-Newtonian Fluid Mech. 74 (1998) 195–245.
[9] J.M. Marchal, M.J. Crochet, J. Non-Newtonian Fluid Mech. 26 (1987) 77–114.
[10] M. Fortin, A. Fortin, J. Non-Newtonian Fluid Mech. 32 (1989) 295–310.
[11] T. Sato, S.M. Richardson, J. Non-Newtonian Fluid Mech. 51 (1994) 249–275.
[12] E.O.A. Carew, P. Townsend, M.F. Webster, J. Non-Newtonian Fluid Mech. 50 (1993) 253–287.
[13] H. Matallah, P. Townsend, M.F. Webster, J. Non-Newtonian Fluid Mech. 75 (1998) 139–166.
[14] J. Sun, M.D. Smith, R.C. Armstrong, R.A. Brown, J. Non-Newtonian Fluid Mech. 86 (1999) 281–307.
[15] D. Rajagopalan, R.C. Armstrong, R.A. Brown, J. Non-Newtonian Fluid Mech. 36 (1990) 159–192.
[16] M.G.N. Perera, K. Walters, J. Non-Newtonian Fluid Mech. 2 (1977) 49–81.
[17] J. Sun, N. Phan-Thien, R.I. Tanner, J. Non-Newtonian Fluid Mech. 65 (1996) 75–91.
[18] R.C. King, M.R. Apelian, R.C. Armstrong, R.A. Brown, J. Non-Newtonian Fluid Mech. 29 (1988) 147–216.
[19] P.J. Roache, Computational Fluid Dynamics, Hermosa Publishing, Albuquerque, 1982.
[20] P.J. Oliveira, F.T. Pinho, Numerical Heat Transfer, Part B 35 (1999) 295–315.
[21] R.B. Bird, R.C. Armstrong, O. Hassager, Dynamics of Polymeric Liquids, Vol. 1, Fluid Mechanics, 2nd Edition, Wiley, New York, 1987.
[22] R.S. Rivlin, Q. Appl. Math. 15 (1957) 212–215.
[23] R.B. Bird, C.F. Curtiss, J. Non-Newtonian Fluid Mech. 79 (1998) 255–259.
[24] R. Guenette, M. Fortin, J. Non-Newtonian Fluid Mech. 60 (1995) 27–52.
[25] N. Phan-Thien, R.I. Tanner, J. Non-Newtonian Fluid Mech. 2 (1977) 353–365.